pharmaceuticals

MDPI

Article

Pioglitazone Is a Mild Carrier-Dependent Uncoupler of Oxidative Phosphorylation and a Modulator of Mitochondrial Permeability Transition

Ekaterina S. Kharechkina [1], Anna B. Nikiforova [1], Konstantin N. Belosludtsev [1,2], Tatyana I. Rokitskaya [3], Yuri N. Antonenko [3] and Alexey G. Kruglov [1,*]

[1] Institute of Theoretical and Experimental Biophysics, Russian Academy of Sciences, Institutskaya 3, 142290 Pushchino, Russia; katya.kypri@gmail.com (E.S.K.); nikiforanna@yandex.ru (A.B.N.); bekonik@gmail.com (K.N.B.)
[2] Mari State University, pl. Lenina 1, 424001 Yoshkar-Ola, Russia
[3] Belozersky Institute of Physico-Chemical Biology, Lomonosov Moscow State University, 119991 Moscow, Russia; rokitskaya@belozersky.msu.ru (T.I.R.); antonen@belozersky.msu.ru (Y.N.A.)
* Correspondence: krugalex@rambler.ru; Tel.: +7-4967-739107

Abstract: Pioglitazone (PIO) is an insulin-sensitizing antidiabetic drug, which normalizes glucose and lipid metabolism but may provoke heart and liver failure and chronic kidney diseases. Both therapeutic and adverse effects of PIO can be accomplished through mitochondrial targets. Here, we explored the capability of PIO to modulate the mitochondrial membrane potential ($\Delta\Psi_m$) and the permeability transition pore (mPTP) opening in different models in vitro. $\Delta\Psi_m$ was measured using tetraphenylphosphonium and the fluorescent dye rhodamine 123. The coupling of oxidative phosphorylation was estimated polarographically. The transport of ions and solutes across membranes was registered by potentiometric and spectral techniques. We found that PIO decreased $\Delta\Psi_m$ in isolated mitochondria and intact thymocytes and the efficiency of ADP phosphorylation, particularly after the addition of Ca^{2+}. The presence of the cytosolic fraction mitigated mitochondrial depolarization but made it sustained. Carboxyatractyloside diminished the PIO-dependent depolarization. PIO activated proton transport in deenergized mitochondria but not in artificial phospholipid vesicles. PIO had no effect on K^+ and Ca^{2+} inward transport but drastically decreased the mitochondrial Ca^{2+}-retention capacity and protective effects of adenine nucleotides against mPTP opening. Thus, PIO is a mild, partly ATP/ADP-translocase-dependent, uncoupler and a modulator of ATP production and mPTP sensitivity to Ca^{2+} and adenine nucleotides. These properties contribute to both therapeutic and adverse effects of PIO.

Keywords: permeability transition pore; unilamellar vesicles; adenine nucleotide translocase; uncoupling protein; ATP production

Citation: Kharechkina, E.S.; Nikiforova, A.B..; Belosludtsev, K.N.; Rokitskaya, T.I.; Antonenko, Y.N.; Kruglov, A.G. Pioglitazone Is a Mild Carrier-Dependent Uncoupler of Oxida-tive Phosphorylation and a Modulator of Mitochondrial Per-meability Transition. *Pharmaceuticals* **2021**, *14*, 1045. https://doi.org/10.3390/ph14101045

Academic Editors: Thierry Besson and Pascal Marchand

Received: 23 September 2021
Accepted: 11 October 2021
Published: 14 October 2021

1. Introduction

PIO is a member of the thiazolidinedione class of insulin-sensitizing drugs, which are extensively used in the treatment of type 2 diabetes. Its impact on diabetes is linked primarily to the binding and activation of the peroxisome proliferator-activated receptor-γ, which regulates the expression of numerous insulin-responsive genes involved in the control of glucose and lipid metabolism [1]. The results of recent meta-analyses of population studies indicate that PIO efficiently decreases the blood pressure, the level of triglycerides, glycated hemoglobin, and blood glucose in fasting animals, as well as the risk of hypoglycemia [2–4]. Besides, due to its anti-inflammatory, antioxidant, and, perhaps, antibacterial and antifungal properties, PIO is now considered as a promising medicine

for the treatment of a range of pathologic states, including Alzheimer's disease [5], depressive disorder [6], non-alcoholic fatty liver disease [7], renal ischemia-reperfusion injury [8], *Klebsiella pneumoniae* infection [9], fibromyalgia-associated motor dysfunctions [10], respiratory infections (including Coronavirus disease 2019) [11,12], chronic obstructive pulmonary disease [13], cryptococcal meningitis [14], and ischemic outcomes induced by mild traumatic brain injury [15]. The intake of PIO is associated with a decrease in carotid intima-media thickness, a hallmark of atherosclerosis progression [2,16]. Although PIO decreases the probability of myocardial infarction and stroke in patients with clinical manifestations of cardiovascular disease, it does not reduce the all-cause mortality and increases the risk of heart failure [17,18]. Furthermore, PIO significantly raises the frequency of peripheral oedema [2], which may be due to fluid retention but not cardiac dysfunction [19]. What is more, PIO augments the probability of a newly developed chronic kidney disease [20]. Liver dysfunctions, including hepatitis, deregulation of the level of hepatic enzymes, and mixed hepatocellular-cholestatic liver injury, as well as liver failure with or without fatal outcomes, have been reported to be associated with the intake of PIO [21]. Besides, PIO significantly increases the risk of bladder cancer [22] but can display cytotoxic and cytostatic effects on several cancer cell lines [23–26].

Several mechanisms were proposed to explain the cardioprotective effect of PIO: anti-inflammatory effect [24,27], upregulation of mitochondrial antioxidant proteins [28,29], activation of mitochondrial ATP-sensitive K^+ channel [30], induction of peroxisome proliferator-activated receptor gamma/peroxisome proliferator-activated receptor gamma coactivator 1-alpha signaling pathway [29], activation of pro-survival signaling phosphoinositide 3-kinases and P42/44 mitogen-activated protein kinases [31], cycloxygenase-2 and cytosolic phospholipase A2 [32], and inhibition of apoptosis [33]. The mechanisms of the adverse effects of PIO are unclear. According to a recent study, thiazolidinediones (including PIO) can induce toxicological molecular alterations via induction of cytochrome p450s that synthesize cardiotoxic 20-hydroxyeicosatetraenoic acid [34]. However, some evidence indicates that they are mitochondria-dependent and involve apoptosis, ferroptosis, autophagy, and mPTP opening [23,24,33,35–37].

One of the mitochondrial PIO targets is CDGSH iron-sulfur domain-containing protein 1 (mitoNEET) in the outer membrane [38]. MitoNEET transfers the 2Fe-2S cluster to cytosolic apoproteins, such as aconitase and apoferredoxin [39]. MitoNEET plays an important role in the regulation of iron homeostasis [40,41], ferroptosis [41], and mitochondrial biogenesis and network [35,42], oxidative capacity [43], reactive oxygen species production, and autophagy [35,40,44,45]. MitoNEET can be involved in glucose and lipid metabolism since the level of protein expression in pancreatic α- and β-cells regulates insulin secretion, glucose tolerance, and mitophagy [46], while in adipocytes it controls lipid uptake and storage [47,48]. It was shown that PIO stabilizes the 2Fe-2S cluster in mitoNEET [49] and prevents its transfer to apoproteins and iron transport to the mitochondria [50].

Another potential target for PIO in the mitochondria is glyceraldehyde 3-phosphate dehydrogenase (GAPDH), which is a proapoptotic regulator of mitochondrial membrane permeabilization [51]. It was shown that, at high concentrations (>100 μM), PIO inhibits the activity and decreases the expression of GAPDH [52].

The data on the direct effect of PIO on mitochondrial functions are limited. PIO was reported to decrease $\Delta\Psi_m$ and uncouple the oxidative phosphorylation via the upregulation of the uncoupling protein 2 [43,44] and the production of reactive oxygen and nitrogen species [47]. Besides, it was found that PIO decreases state 3 mitochondrial respiration due to the inhibition and disassembly of complex I [23,53] and the inhibition of complex III [54,55]. Other studies did not confirm the uncoupling [54,56] and the inhibition of complexes by PIO [57]. In mitochondria isolated from hepatocytes and human skeletal muscles, PIO inhibited the ATP production [36,58], which may be connected with the stimulation of mPTP opening [36]. Other researchers reported that PIO does not affect the mPTP opening and ATP production [54].

Thus, it is unclear whether PIO is capable of directly modulating mitochondrial functions. At the same time, the structure of the PIO molecule allows reversible protonation (pKa 5.19) [59] and incorporation into the lipid bilayer (octanol-water partition coefficient ~2.3). These properties are inherent in conventional protonophores, which can penetrate through membranes both in neutral (protonated) and anionic forms [60]. Therefore, the aims of the present study were to assess the protonophoric and uncoupling effects of PIO in mitochondria and artificial lipid membranes and to clarify the effect of PIO on the mPTP opening in different models in vitro.

2. Results

2.1. PIO Acts as a Low-Efficient Uncoupler in Isolated Mitochondria

First, we examined the effect of PIO on $\Delta\Psi_m$ and oxidative phosphorylation (Figure 1). As follows from the figure, PIO reduced the accumulation of rhodamine 123 in mitochondria (Figure 1B) and induced a release of accumulated tetraphenylphosphonium (TPP^+) (Figure 1A), indicating a decrease in $\Delta\Psi_m$. The determination of $\Delta\Psi_m$ in the presence of PIO (Figure 1C,D) revealed a temporary dose-dependent decrease (up to 50 mV) in membrane potential with a subsequent slow return to control values (Figure 1C). PIO was a weaker proton gradient disrupter than carbonyl cyanide p-(trifluoromethoxy)phenyl-hydrazone (FCCP) and 2,4-dinitrophenol (DNP) (by two to three orders of magnitude and several times, respectively) (Figure 1C, insert). Besides, PIO strongly decreased $\Delta\Psi_m$ in the presence of substrates of complex I compared to substrates of complex II. Even at a low concentration (2.5–20 μM), PIO noticeably reduced the efficiency of oxidative phosphorylation (Figure 1D and insert). It stimulated state 2 respiration and decreased the respiratory control coefficient (RC) and, though only slightly, the rate of state 3 respiration. Thus, PIO acts as a low-efficient protonophoric uncoupler, such as natural bile acids [61].

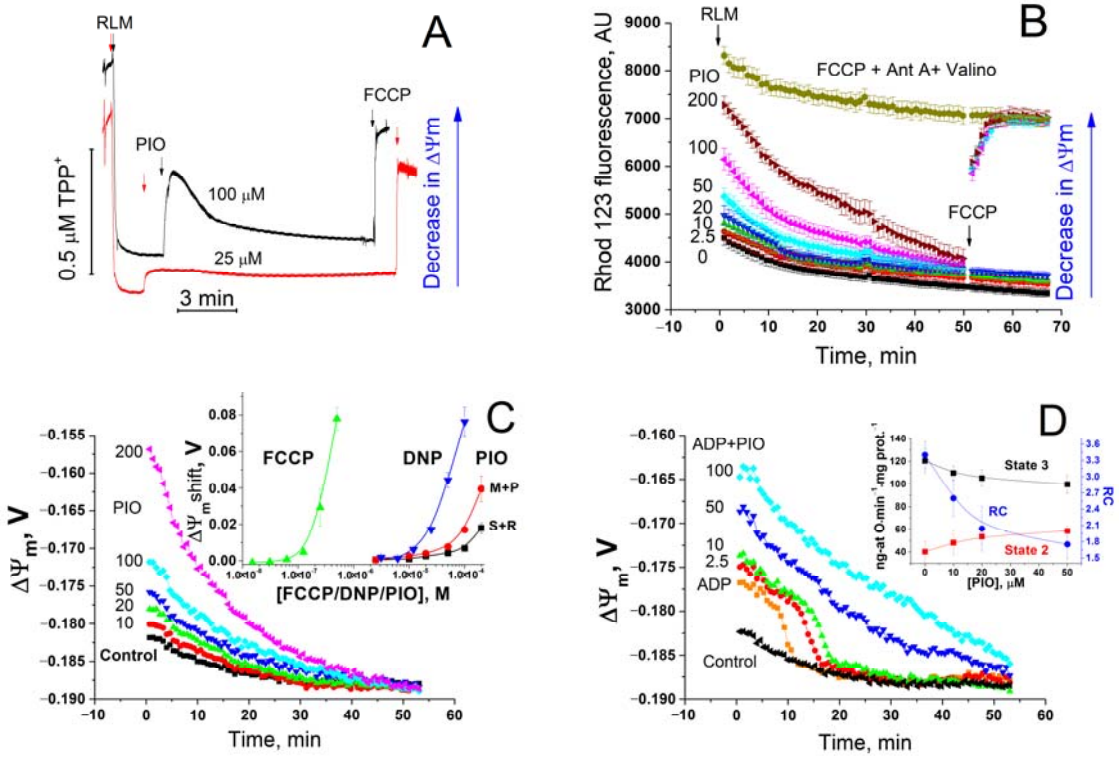

Figure 1. Effect of PIO on $\Delta\Psi_m$ and the coupling of mitochondria. (**A**,**B**) Assessment of the effect of PIO on $\Delta\Psi_m$ using TPP^+ (**A**) and rhodamine 123 (Rhod 123, (**B**)). (**C**,**D**) Effect of PIO on $\Delta\Psi_m$ in mitochondria in the resting state (**C**) and during the ADP phosphorylation (**D**). (**A**) Rat liver mitochondria (RLM) (1 mg prot./mL) were placed in a standard incubation medium supplemented with 5 mM K^+-succinate, 1 mM EGTA, rotenone (2 μg/mL), and 1 μM TPP^+. Arrows show the addition of 25 or 100 μM PIO and 500 nM FCCP. (**B**–**D**) A mitochondrial suspension (0.75 mg/mL) supplemented with

respiratory substrates, 1 mM EGTA, and 330 nM rhodamine 123 was placed in wells with 1% dimethyl sulfoxide (DMSO) (vehicle control) or PIO at indicated concentrations (μM) (**B**–**D**), 500 nM FCCP, antimycin A (2.5 μg/ml), and valinomycin (25 ng/mL) (**B**), and 2 mM ADP (**D**) just before measurements. Everywhere, except the curve designated "M+P" (5 mM malate + 5 mM pyruvate), the respiratory substrate was 5 mM K^+-succinate with the addition of rotenone (2 μg/mL). Numbers on curves are the means ± S.E.M. (n = 3) of one representative experiment of three identical experiments. (**B**) Where indicated, 500 nM FCCP was added to wells with 50, 100, and 200 μM PIO to calibrate the signal. Insert in panel (**C**) shows a shift in $\Delta\Psi_m$ caused by FCCP, DNP, and PIO after 5 min of incubation. Insert in panel (**D**) shows the effect of PIO on the respiration rate in state 2 and state 3 and the respiratory control (RC) coefficient. In inserts, numbers on curves are the means ± S.E.M. of three independent experiments (n = 9 (**C**) and 3 (**D**)).

2.2. PIO Modulates the Sensitivity of the Permeability Transition Pore to Regulators

It was reported that PIO stimulates the opening of mPTP [36]. However, mPTP opening can disrupt the transmembrane proton gradient and uncouple the respiration and oxidative phosphorylation. Therefore, we explored the effect of PIO on the mPTP opening in the mitochondria in different experimental conditions. Figure 2 shows that PIO (10–100 μM) neither induced the ionic permeability of the inner mitochondrial membrane (IMM) in KCl-based medium (Figure 2A) nor markedly influenced the mPTP opening by a single addition of Ca^{2+} (Figure 2A, insert). At the same time, PIO negligibly affected the Ca^{2+} uptake rate (Figure 2D, insert) but drastically reduced the mitochondrial Ca^{2+} retention capacity (Figure 2D) (mitochondria were exposed to 30 μM pulses). Besides, PIO noticeably weakened the inhibition of the mPTP opening by added ADP (Figure 2B) and ATP (Figure 2C) (ADP and ATP are strong natural mPTP inhibitors, which can be present in the cytosol of living cells at millimolar concentrations). Thus, PIO does not induce the mPTP opening itself but can modulate the mitochondrial susceptibility to mPTP regulators, Ca^{2+} and ATP/ADP, under certain conditions.

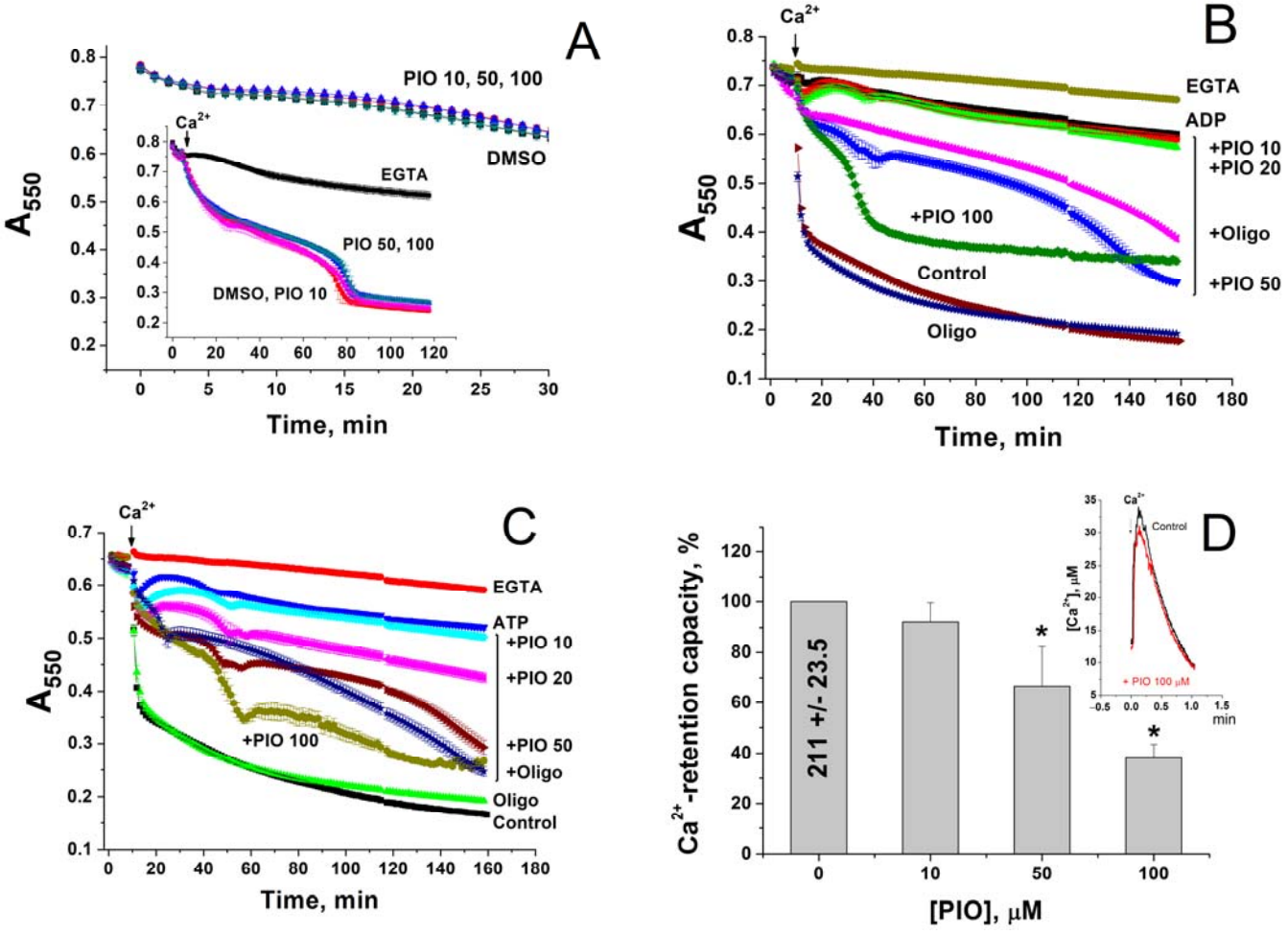

Figure 2. PIO increases mitochondrial sensitivity to Ca^{2+} and decreases the protective effect of mPTP inhibitors, ATP and ADP. (**A**–**C**) Ca^{2+}-dependent mitochondrial swelling in the presence of PIO and ATP/ADP. (**D**) Effect of PIO on the Ca^{2+}-retention capacity of mitochondria. (**A**–**C**) Mitochondrial suspension (0.75 mg prot./mL) supplemented with 5 mM K^+-succinate (plus 2 μg/mL rotenone) and, where shown, 2 mM ADP (**B**) and 2 mM ATP (**C**) (pH 7.4) were placed in wells with indicated additions: 1 mM EGTA, 1% DMSO, 10–100 μM PIO, and 10 μg/mL oligomycin (Oligo). The arrow shows the addition of 50 μM Ca^{2+}. Representative data of three similar experiments are shown. Points on traces are the means ± S.E.M. (n = 3). (**D**) Ca^{2+}-retention capacity equal to 100% corresponds to 210.9 ± 23.45 nmol Ca^{2+}/mg protein. Values in columns are means ± S.E.M. (n = 3) of three independent experiments. The asterisk shows the significant difference from the vehicle control ($p < 0.05$). The insert shows the kinetics of accumulation of 30 μM Ca^{2+} in the absence (Control) and in the presence of 100 μM PIO.

2.3. PIO Decreases the Capability of Mitochondria to Phosphorylate ADP in the Presence of Ca^{2+}

Mitochondria within a living cell permanently exist in intermediate 3–4 metabolic state and are exposed to repeating Ca^{2+} pulses from endoplasmic/sarcoplasmic reticulum and the extracellular space, particularly in excitable tissues. We examined the effect of PIO on the capacity of mitochondria to maintain the level of endogenous ATP and ATP production after a single Ca^{2+} pulse (Figure 3). The release of ATP from intact mitochondria was traced using a 20% solution of a luciferin-luciferase reagent (without lysis buffer), which rapidly oxidizes external ATP and generates chemiluminescence. It should be noted that the luminescence produced by luciferase in the presence of ATP (left scale line) was 20 times more intensive than in the presence of ADP (right scale line) [62]. The relatively low but sustained luminescence in a mitochondrial suspension was interpreted as a continuous exchange of small quantities of ATP for ADP/AMP between the medium and mitochondria, since it was completely inhibited by oligomycin (Figure 3A). As it follows from the figure, 500 μM ADP caused a strong increase in the chemiluminescence, which comprised two constituents: (1) oligomycin-sensitive, dependent on the ATP generated by F_oF_1-ATPase, and (2) oligomycin-insensitive, dependent on ADP and ATP produced by adenylate kinase in the intermembrane space. PIO decreased the ADP-stimulated ATP release in a dose-dependent manner. Ca^{2+} further diminished the ATP production, which transiently became negligible at 50 μM PIO. Moreover, PIO reduced the level of matrix ATP, which can be released by the small Ca^{2+}-activated mitochondrial carrier protein (SCaMC) in exchange for inorganic phosphate (Figure 3B) [63]. Hence, PIO strongly decreases the level of matrix ATP and reduces the capacity of the mitochondria for ATP production after a pulse of Ca^{2+}.

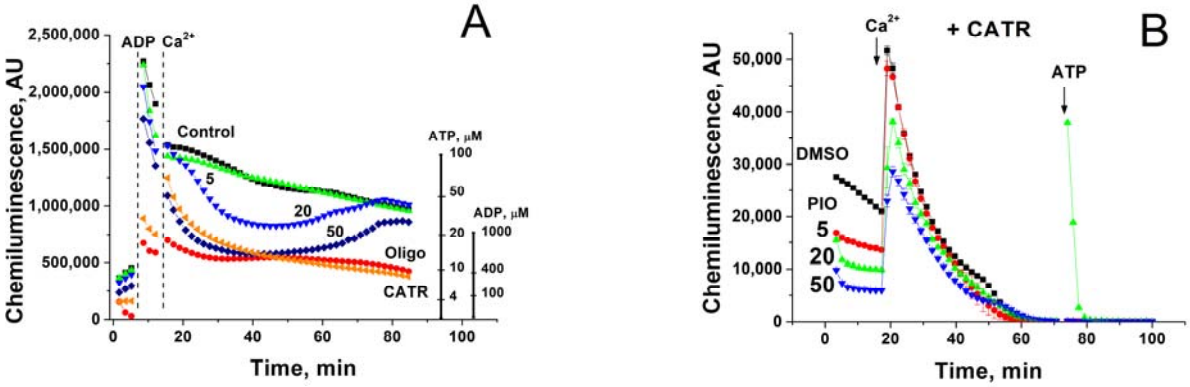

Figure 3. Effect of PIO on the capability of mitochondria to support ATP production in the presence of Ca^{2+} (**A**) and on the level of matrix ATP (**B**). Mitochondria (0.2 (**A**) and 0.5 mg prot./mL (**B**)) were placed in the standard incubation medium, which contained a 20% solution of a luciferin-luciferase reagent, 5 mM K^+-succinate, 2 μg/mL of rotenone, 10 μM EGTA, and, where indicated, 5–50 μM PIO, 1 μM CATR, and 10 μg/mL oligomycin (Oligo). Vertical dashed lines (**A**) or arrows (**B**) show the addition of 500 μM ADP, 50 μM Ca^{2+}, and 5 μM ATP standard (to calibrate the chemiluminescent signal). Representative data of three separate experiments are shown. Traces are the means for three wells.

2.4. Effect of PIO on the Permeability of the Inner Mitochondrial and Lecithin Liposomal Membranes to Protons

The molecular structure of PIO indicates that it may be reversibly protonated as conventional protonophores, such as FCCP or carbonyl cyanide m-chlorophenyl hydrazone (CCCP) (Figure 4A). Therefore, we studied the effect of PIO on the pH value in large unilamellar lecithin vesicles loaded with the fluorescent pH probe pyranine. Figure 4B shows the kinetics of dissipation of a pre-formed pH gradient on membranes of liposomes after the addition of PIO (red, green, and blue curves) or CCCP (pink curve). Black and brown curves show the control and vehicle control (15 μL DMSO), respectively. In contrast to the effect of CCCP, the addition of different concentrations of PIO (10 μM, red; 50 μM, green; 75 μM, blue) did not lead to an increase in the signal of pyranine (Figure 4B). It can be concluded that PIO is not able to induce proton transport in a pure lipid system.

We examined whether the effect of PIO on $\Delta\Psi_m$ in mitochondria is connected with the activation of proton inward transport or with other reasons. Figure 4C shows that PIO accelerated the swelling of deenergized mitochondria in NH_4NO_3-based medium in a dose-dependent manner. This indicates that PIO, indeed, increased the permeability of the IMM to protons. PIO was a proton carrier three orders of magnitude weaker than FCCP but slightly more efficient than free palmitic acid (Figure 4D). Hence, PIO can transport protons in mitochondria but cannot do so in/out of liposomes.

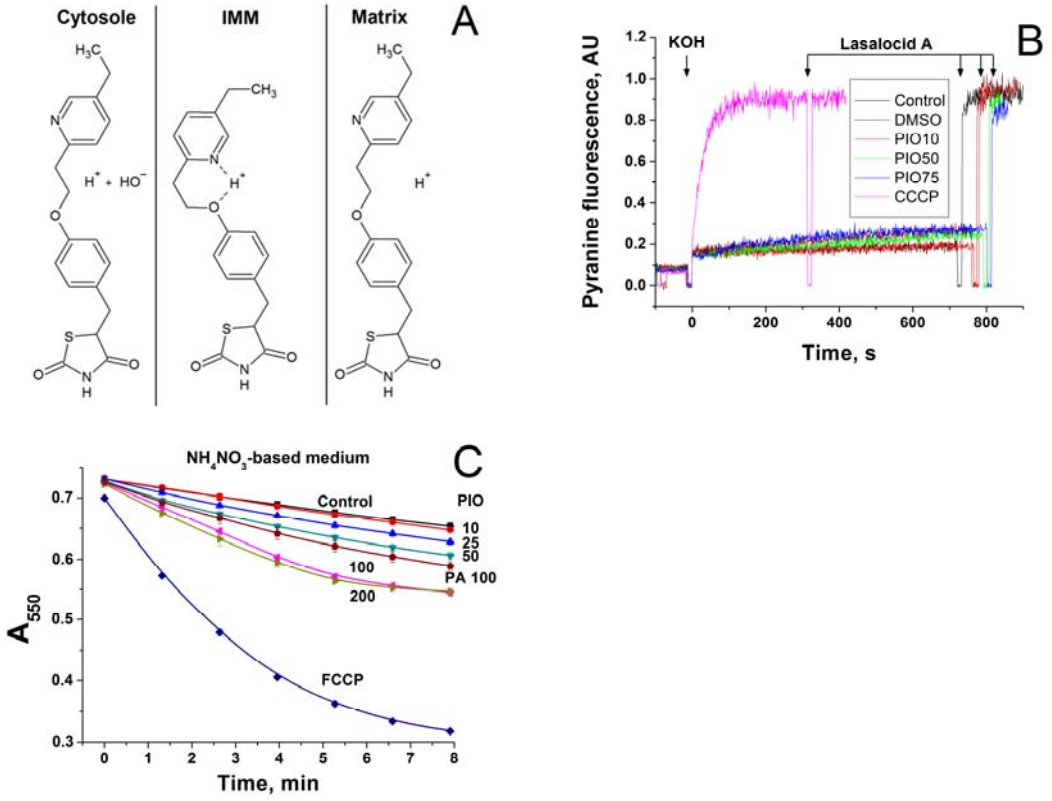

Figure 4. Mechanism of transmembrane proton transport by PIO. (**A**) Possible mechanism of proton transport by PIO across the IMM. (**B**) Comparison of CCCP- and PIO-mediated proton fluxes through liposomes loaded with the pH probe pyranine. The inner liposomal pH value was estimated from the pyranine fluorescence intensity measured at 505 nm upon excitation at 455 nm. Lasalocid A (1 μM) was added approximately at 800 s to equilibrate pH. PIO concentrations were 10 μM, red curve; 50 μM, green curve; 75 μM, blue curve. CCCP concentration was 1 μM (pink curve). Lipid concentration was 20 μg/mL, T = 15 °C. Other conditions: see Materials and Methods Section. The proton flux was initiated by an alkaline pH shift from pH 6 to pH 8, which was caused by the addition of the previously determined aliquot of KOH. In the presence of the protonophores, the pyranine fluorescence gradually increased, indicating the alignment of the pH values inside and outside liposomes due to proton transfer mediated by a protonophore. (**C**,**D**) Effect of PIO, palmitic acid, and FCCP on the swelling of deenergized mitochondria in NH_4NO_3-based medium. Mitochondria (0.75 mg prot./mL) were added to NH_4NO_3-based medium supplemented with rotenone (2.5 mg/mL), and 1 min later, the suspension was placed

in the wells of a plate that contained PIO, sodium palmitate (PA), and FCCP at indicated concentrations. (**C**) Standard curves of mitochondrial swelling. (**D**) Initial rates of mitochondrial swelling during the first 3 min of incubation. Points are the means ± S.E.M. of three independent experiments (n = 9).

2.5. Role of Mmitochondrial Carriers in PIO-Dependent Depolarization of Mitochondria

Mitochondrial carriers are known to contribute to mitochondrial depolarization caused by fatty acids and other reversibly protonated compounds. The ADP/ATP carrier (ANT) facilitates the transport of fatty acid anions from the inner to the outer leaflet of the IMM and, therefore, reinforces the uncoupling of oxidative phosphorylation [64,65]. Uncoupler proteins 1–3 (UCPs) possess a similar activity [65,66]. We assessed the effect of the ANT and UCPs inhibitors carboxyatractyloside (CATR) and GDP on mitochondrial depolarization caused by PIO and conventional protonophores DNP and FCCP. Figure 5A shows that CATR plus GDP diminished the positive shift in $\Delta\Psi_m$ (depolarization of the inner membrane) by PIO by 1–2 (100 μM PIO) and 3–5 mV, temporarily up to 10 mV (200 μM PIO), i.e., ~by 50%. The relative effect of DNP was less sensitive to CATR plus GDP: the decrease in the positive shift was up to 15 mV (15–20%) depending on the DNP concentration and incubation time (Figure 5B). In contrast, CATR and GDP had a minor effect on the FCCP-dependent depolarization (not shown). The analysis of the effects of CATR, GDP, and their combination on the average PIO-dependent positive shift in $\Delta\Psi_m$ demonstrated that both CATR alone and its combination with GDP reduced the shift to a similar extent (Figure 5C). GDP alone did not attenuate the mitochondrial depolarization. Similar results were obtained with DNP (Figure 5D) (Figure 5D shows changes in DNP-dependent $\Delta\Psi_m$ shift (Control, dashed line) caused by CATR and GDP). Thus, in liver mitochondria, ANT contributes to PIO- and DNP-induced mitochondrial uncoupling, while UCPs do not.

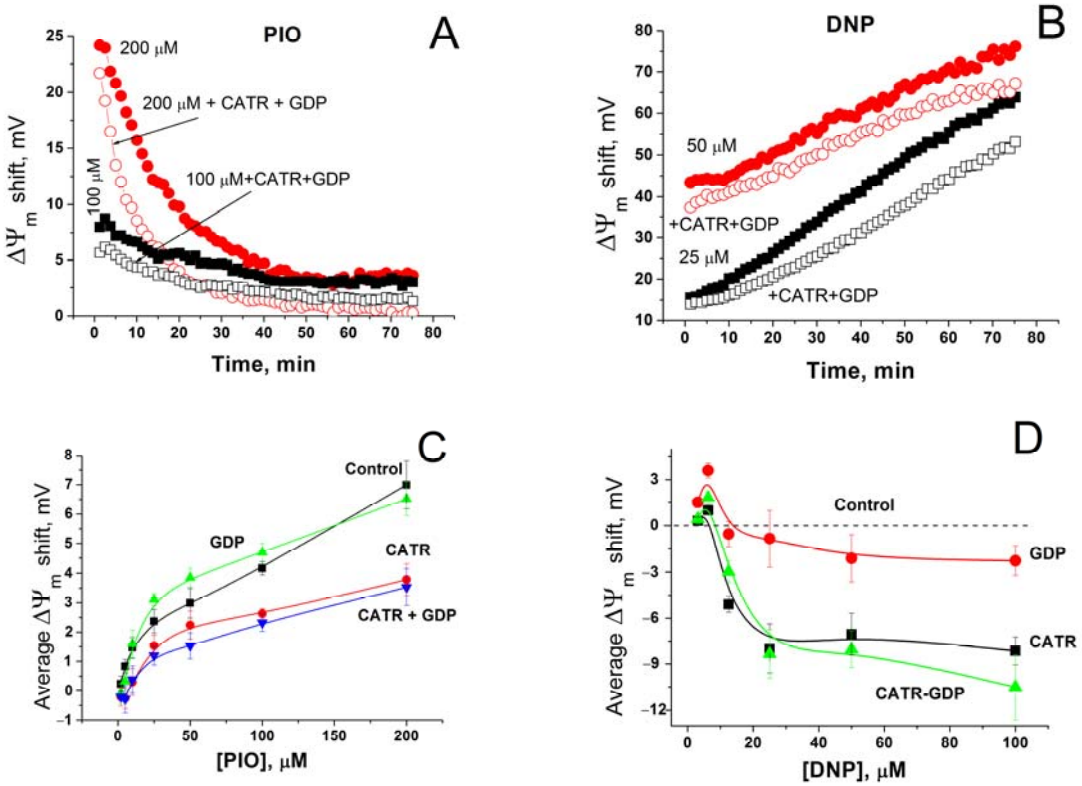

Figure 5. Effect of inhibitors of ANT and UCPs on the shift in $\Delta\Psi_m$ caused by PIO and DNP. Incubation medium contained indicated concentrations of PIO and DNP, and, where shown, 1 mM GDP and 2 μM CATR. (**A**,**B**) Dynamics of $\Delta\Psi_m$ changes (decrease) in relation to control (1% DMSO). The data of one representative experiment of three similar experiments are shown. Values on traces are the means for three wells. (**C**) Effect of GDP and CATR on the average PIO-dependent shift in $\Delta\Psi_m$. Each point on the curves is an average $\Delta\Psi_m$ shift defined as a mean ± S.E.M. for 60 points of experimental

curves (such as in Panel (**A**)) for three individual experiments (n = 180). (**D**) Changes in the DNP-dependent $\Delta\Psi_m$ shift caused by CATR and GDP in relation to DNP alone (Control).

2.6. PIO Causes Mild Mitochondrial Depolarization in Intact Cells

We examined whether the effect of PIO on $\Delta\Psi_m$ is preserved in intact cells. Figure 6 demonstrates that 30-min incubation of cells with 50 (Figure 6B,E) and 200 μM PIO (Figure 6C,E) significantly increased the portion of isolated thymocytes with depolarized mitochondria in comparison with the control (Figure 6A,E). However, the effect was substantially less pronounced than the effect of 500 nM FCCP (Figure 6D,E). Thus, PIO can act as a mild depolarizing agent in mitochondria of intact cells.

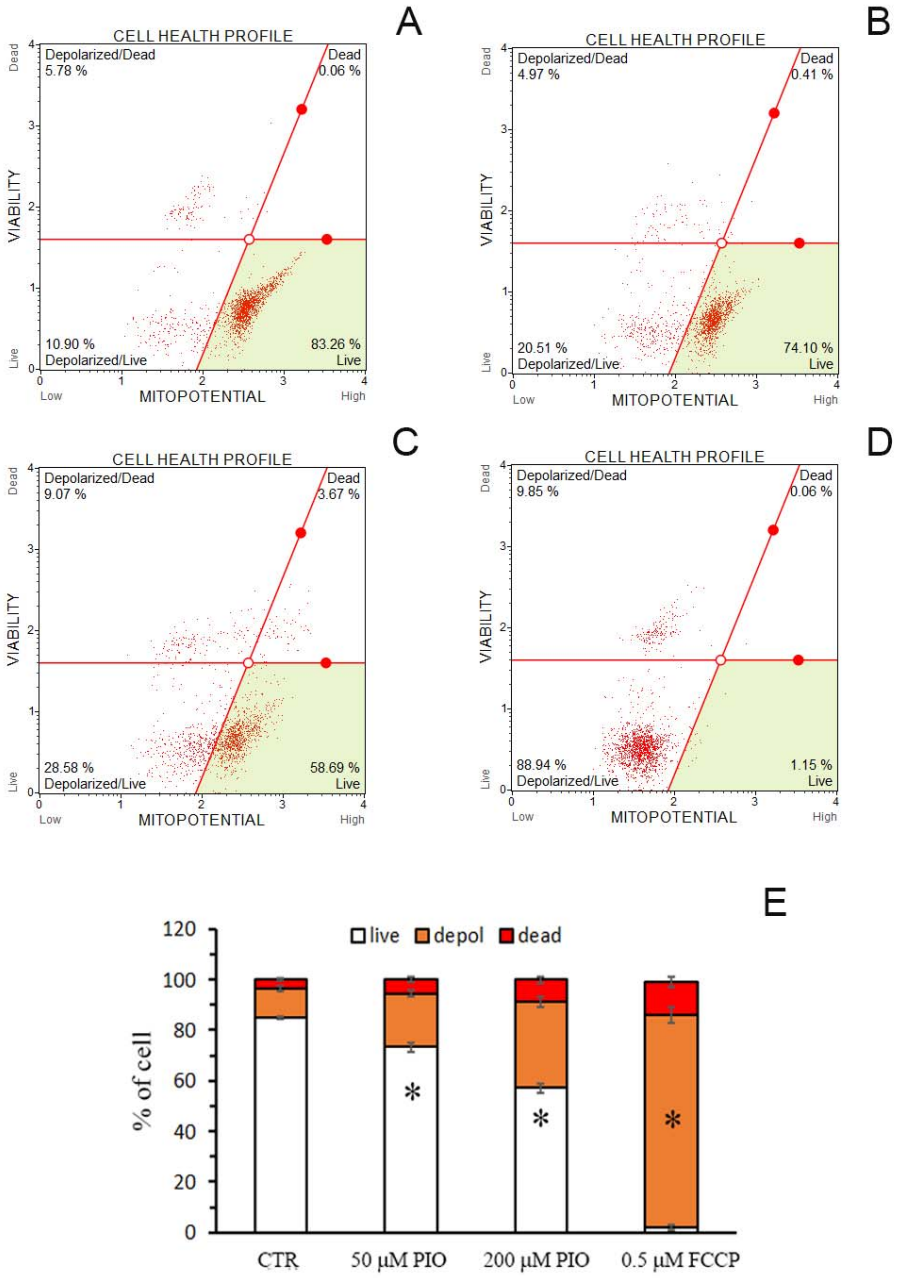

Figure 6. PIO decreases $\Delta\Psi_m$ in isolated intact thymocytes. (**A**–**D**) Typical plots obtained in the absence of additions (**A**, Control), in the presence of 50 (**B**) and 200 μM PIO (**C**), and 500 nM FCCP (**D**). (**E**) The portion of depolarized cells in different experimental groups (means ± SEM, n = 3). * Statistically significant ($p < 0.05$) differences from control (without PIO).

2.7. Effect of PIO on $\Delta\Psi_m$ in Isolated Mitochondria and Mitochondria in Nuclei-Free Liver Homogenate

In isolated mitochondria, PIO-dependent depolarization was transient (see Figures 1, 4 and 5): the higher the PIO concentration was, the higher the rate of the loss of the effect. Since PIO is poorly soluble in water, one can assume that, at high concentrations, PIO forms suspension, which decreases the effective concentration of PIO and deteriorates its protonophoric effect. However, the cytosol of living cells comprises constituents that increase solubility and facilitate the transport of poorly soluble compounds [67,68]. Therefore, we compared the rate of restoration of $\Delta\Psi_m$ in the presence of PIO in a standard mitochondrial suspension and a suspension that contained mitochondria- and nuclei-free rat liver homogenate (RLH) diluted to a final concentration of 5 (Figure 7B,D) and 15 mg prot./mL (Figure 7C,D).

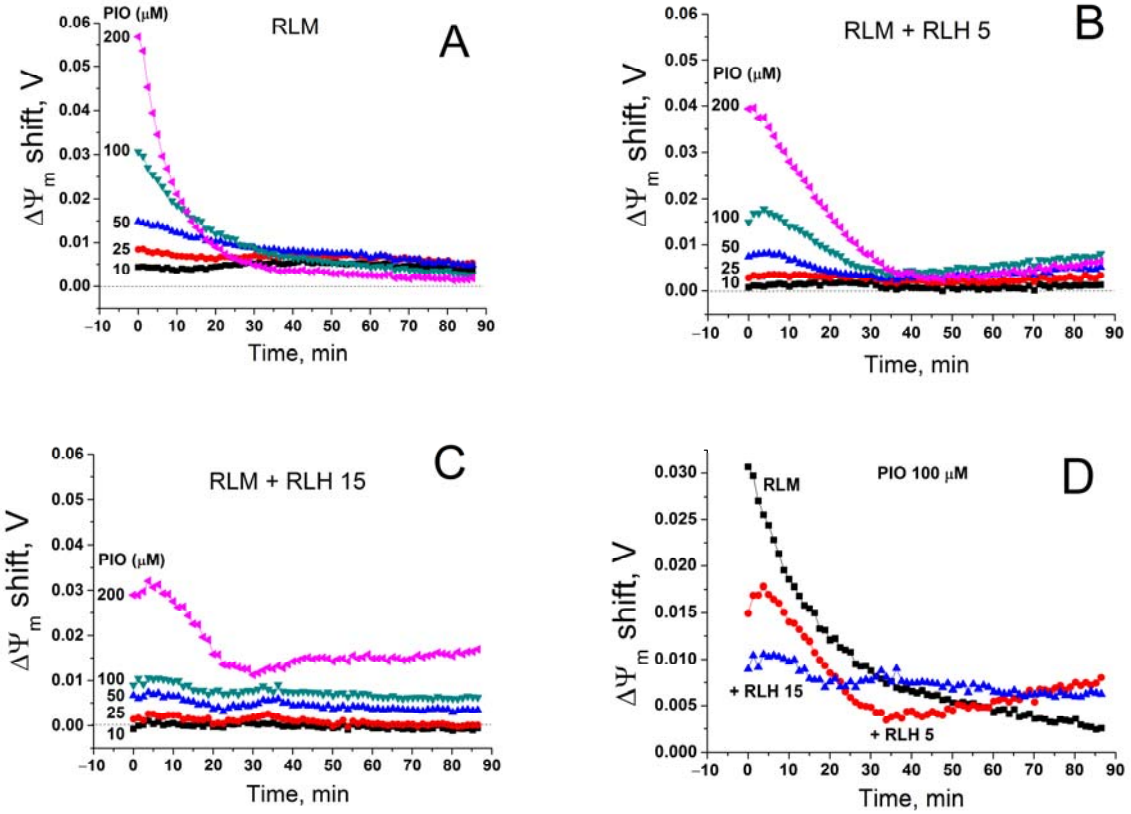

Figure 7. Effect of a cytosolic fraction (RLH) on PIO-dependent changes in $\Delta\Psi_m$. Just before measurements, mitochondria alone (RLM) (0.75 mg prot./mL) (**A**,**D**) or in combination with 5 (**B**,**D**) and 15 mg prot./mL (**C**,**D**) of RLH were added to a standard incubation medium supplemented with 5 mM K^+-succinate, 1 mM EGTA, rotenone (2.5 μg/mL), and 330 nM rhodamine 123, and then transferred to the wells of a 96-well plate, which contained 1% DMSO (Control), 10–200 μM PIO, or 500 nM FCCP, antimycin A (2.5 μg/mL), and valinomycin (25 ng/mL). Traces are the differences in $\Delta\Psi_m$ between PIO- and DMSO-containing samples in one representative experiment of three similar experiments.

As it follows from Figure 7, RLH diminished the initial PIO-dependent positive shift in $\Delta\Psi_m$ (deteriorated the maximum depolarization) in a dose-dependent manner. Simul-

taneously, the depolarization induced by PIO at high concentrations became more sustainable (Figure 6C,D). Hence, cytosolic components, presumably, did not increase the solubility and the effective concentration of PIO but rather acted as a PIO buffer.

3. Discussion

The study confirmed that PIO can act as an uncoupler of oxidative phosphorylation, though much less efficient than FCCP (Figures 1 and 5) and 2,4-dinitrophenol [69], but equally or more efficient than fatty (Figure 4) and bile acids [61,70]. However, despite the octanol-water partition coefficient of 2.3 and the pKa of 5.19 [59], PIO per se cannot operate either as a classical protonophore (Figure 4) or as a K^+ ionophore (Figure 2) in mitochondrial and artificial lipid membranes. Nevertheless, PIO-dependent mitochondrial depolarization is associated with the activation of inward proton transport (Figure 4C,D).

It was established three decades ago that ANT can translocate fatty acid anions across the IMM, which strengthens the uncoupling effect of exogenous and endogenous fatty acids [64,71]. Substrates and inhibitors of ANT suppress the protonophoric effect of fatty acids [65,72]. UCPs, a family of proteins structurally related to ANT, can also mediate the fatty acid-dependent depolarization of the IMM and mitochondrial uncoupling [73]. According to recent findings, UCP2 possesses the activity of the fatty acid flippase, which is essential for proton conductance [66]. GDP interferes with the binding of fatty acids to UCP1 and 2 and suppresses proton currents [73]. Mitochondrial uncoupling by DNP is known to be partially dependent on ANT, while the effect of FCCP is carrier-independent [64]. Novel data indicate that both recombinant ANT1 and UCP1-3 considerably increase the protonophoric effect of DNP in planar bilayer lipid membranes and that arginine 79 of ANT1 is essential for DNP binding and translocation [65]. Here, we demonstrated that, in liver mitochondria, ANT considerably contributes to PIO-dependent mitochondrial depolarization and uncoupling (Figure 5). The role of UCP proteins demands further clarification since neither PIO- nor DNP-dependent depolarization was sensitive to the UCP inhibitor in liver mitochondria, which may be due to the low level of the carriers but not to an inability to transport PIO per se [65]. Thus, PIO-dependent mitochondrial depolarization and uncoupling is ANT-mediated, at least partially.

The interaction of PIO with ANT, an important regulator of mPTP, can explain the slight inhibition of state 3 respiration (Figure 1), the reduction of the mitochondrial Ca^{2+}-retention capacity, and the cancellation of the suppression of mPTP by adenine nucleotides (Figure 2). Besides, by activating the inward proton transport, PIO can decrease the pH value in the mitochondrial matrix, which promotes the mPTP opening [74]. Another mechanism for facilitation of mPTP opening may be connected to the depletion of matrix ATP (Figure 3) via the Ca^{2+}-activated SCaMC-mediated pathway [62,63,75].

A short duration of the PIO-dependent depolarization of isolated mitochondria in suspension (Figures 1, 4 and 5) is, presumably, connected with poor solubility in water (4–6.5 μg/mL or 11–16.5 μM) [67,76], but not with the glutathione-s-transferase-dependent inactivation of PIO, as it was shown for other uncouplers [77], since GSH had a negligible effect on the depolarization (not shown).

In living cells, however, the effect of PIO could be long-lasting. Indeed, the cytoplasm contains various compounds capable of acting as co-solvents and increasing the solubility and free concentration of PIO tens and hundreds of times [67]. Alternatively, multiple cytosolic proteins and systems facilitate the storage and transport of poorly soluble compounds [68]. The data obtained are in favor of the second mechanism, since the cytosolic fraction decreased the strength but increased the duration of PIO-dependent mitochondrial depolarization (Figure 7), i.e., acted as a PIO buffer. Thus, one can expect that PIO-dependent mitochondrial depolarization will be mild (Figure 6) but sustained or even permanent in prolonged treatment in situ or therapy and in vivo.

The data obtained can help one explain some of the adverse effects of PIO in various organs and systems (Figure 8). The increased risk of heart failure in patients with cardiovascular disease [17] may be connected with the effect of PIO on the efficiency of ATP

production under conditions of repeating Ca^{2+} pulses (Figure 3). In addition, the slow release of fluid, peripheral oedema, development of chronic kidney disease, and liver dysfunction promoted by PIO [2,19–21] can be attributed to insufficient production of ATP for ion pumps and exchangers in the plasma membrane. Moreover, the reduction of the mitochondrial Ca^{2+}-retention capacity and the cancellation of the suppression of mPTP by adenine nucleotides (Figure 2) can be a reason for the toxicity of PIO in several cell lines [23–26]. At the same time, the reduction of the risk of myocardial infarction and stroke in patients with clinical manifestation of cardiovascular disease might be connected with long-term effects of PIO, such as the regulation of autophagy and mitochondrial quality control (Figure 8) [33]. Further, mild mitochondrial uncoupling and the activation of glucose and fat metabolism should contribute to the antidiabetic and anti-atherosclerotic action of PIO [2,16,78]. Indeed, another uncoupler, DNP, was successfully applied for the correction of glucose and lipid metabolism in animals and humans [79,80] and is now considered as a promising medicine for the treatment of a range of pathologic states [69].

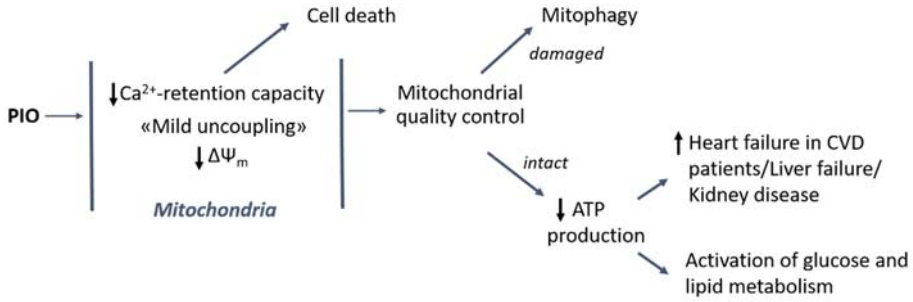

Figure 8. Contribution of uncoupling and mPTP-modulating effects of PIO to its healing and harmful action in the cell and the organism. CVD: cardiovascular disease.

4. Materials and Methods

4.1. Materials

ATP Kit SL (144-041) was purchased from BioThema AB (Haninge, Sweden). ADP (sodium salt) (A2754), ATP (disodium salt hydrate) (A7699), antimycin A (A8674), bovine serum albumin (BSA) (A7030), FCCP (C2920), CATR (C4992), DMSO (276855), DNP (D198501), GDP (sodium salt) (G7127), 4-(2-hydroxyethyl)piperazine-1-ethanesulfonic acid (HEPES) (H3375), palmitic acid (P0500), PIO (hydrochloride) (E6910), rhodamine 123 (R8004), rotenone (R8875), sucrose (S7903), succinate (S3674), TPP^+ (chloride) (218790), Trizma Base (93352), and valinomycin (94675) were purchased from the Sigma-Aldrich Corporation (St. Louis, MO, USA). Ethylene glycol-bis(2-aminoethylether)-N,N,N′,N′-tetraacetic acid (EGTA) (A0878,0025) was from PanReac AppliChem (Darmstadt, Germany). Other chemicals were of analytical grade and were purchased from local suppliers (Moscow, Russia).

4.2. Isolation of Rat Liver Mitochondria and Preparation of the Cytosolic Fraction of Liver Homogenate

All manipulations with animals before the isolation of the liver were performed in accordance with the Helsinki Declaration of 1975 (revised in 1983), national requirements for the care and use of laboratory animals, and protocol 9/2020 of 17.02.2020 approved by the Commission on Biological Safety and Bioethics at the ITEB RAS.

Rat liver mitochondria were isolated by a standard differential centrifugation procedure [81]. Adult male Wistar rats were killed by cutting the neck after anesthesia with CO_2. The homogenization medium contained 220 mM mannitol, 70 mM sucrose, 10 mM HEPES (pH adjusted to 7.4 with Trizma Base), 1 mM EGTA, and 0.05% BSA. The pellet

was washed three times with a medium devoid of EGTA and BSA. Final pellets were resuspended in this medium to yield 60–70 mg protein/mL. Measurements were performed at 37 °C in KCl-based medium (125 mM KCl, 20 mM sucrose, 10 mM HEPES (pH adjusted to 7.3 with Trizma Base), 2 mM KH_2PO_4, 2 mM $MgCl_2$, and 10 μM EGTA) supplemented with 5 mM potassium succinate and rotenone (2 μg/mL), unless otherwise indicated. Other experimental details are provided in figures and figure legends. The intactness of isolated mitochondria was assessed as described previously [82].

The cytosolic fraction of liver homogenate (mitochondria- and nuclei-free RLH) was prepared as follows. The liver (1 g) was homogenized in the standard homogenization medium devoid of BSA. The homogenate was centrifuged 700 g × 15 min and 15,000 g × 20 min. Pellets were discarded at each step. The resulting RLH was kept on ice until use.

The total protein in mitochondrial and cytosolic fractions was determined by the Biuret method using BSA as a standard [83].

4.3. Measurements of the Oxygen Consumption Rate

Mitochondrial respiration was measured using an oxygen Clark-type electrode in a temperature-controlled electrode chamber connected to a computerized recording system, Record 4 (Institute of Theoretical and Experimental Biophysics, Russian Academy of Sciences (ITEB-RAS), Russia). Mitochondria (1 mg/mL) were incubated at 25 °C in standard medium supplemented with 5 mM succinate in the presence of rotenone (2 μg/mL). In order to assess state 3 and state 4 respiration rates, 200–500 μM ADP was added to mitochondria respiring in the presence of substrates (state 2). The RC coefficient was defined as the ratio of the respiration rate in state 3 to the rate in state 4.

4.4. Measurements of $\Delta\Psi_m$ in Isolated Mitochondria

$\Delta\Psi_m$ across the IMM was measured using the $\Delta\Psi_m$-sensitive fluorescent dye rhodamine 123 and a plate reader Infinite 200, Tecan (Grödig, Austria). Standard incubation medium contained respiratory substrates, 1 mM EGTA, 330 nM rhodamine 123, and, where indicated, 2 mM ADP, 1 mM GDP, 2 μM CATR, and PIO, FCCP, and RLH at different concentrations. In order to calibrate the fluorescent signal, each experimental series contained samples with a cocktail of respiratory inhibitors and ionophores, which disrupt ionic gradients across the IMM (500 nM FCCP, antimycin A (2.5 μg/mL), and valinomycin (25 ng/mL)) [84]. $\Delta\Psi_m$ was calculated using the Nernst equation assuming that: (1) the matrix volume is equal to 1 μL/mg protein (liver mitochondria), (2) the fluorescence of rhodamine 123 is directly proportional to the concentration in solution and is totally quenched upon the accumulation in mitochondria, and (3) initial fluorescence in samples with a cocktail of respiratory inhibitors and ionophores corresponds to 300 nM rhodamine 123.

Alternatively, $\Delta\Psi_m$ was assessed using a TPP^+-selective electrode (Niko Analyt, Russia) connected to a computerized recording system, Record 4 (ITEB RAS). The electrode was calibrated with known amounts of TPP^+ at the beginning of each experimental series.

4.5. Measurements of $\Delta\Psi_m$ in Isolated Thymocytes

Thymocytes were isolated from two thymuses of male Wistar rats (90–110 g) in accordance with a known method [85]. Medium containing 145 mM NaCl, 5.6 mM KCl, 10 mM glucose, and 8 mM Mops-KOH (pH 7.4) was used to isolate, wash, suspend, and incubate the cells. In control samples, the cell survival was at least 90%. All experiments with cells were carried out for 3 h; in this case, the cells retained similar viability and mitochondrial potential, as assessed by flow cytometry using a Muse Cell Analyzer (Merck Millipore, Burlington, MA, USA).

The mitochondrial potential was assessed by using a Muse MitoPotential Kit (MCH100110, Merck Millipore, Burlington, MA, USA) in order to determine the percentages of cells exhibiting a change in mitochondrial polarization. All assays were performed strictly according to the manufacturer's protocols.

4.6. Recording of the Permeabilization of Mitochondrial Membranes

The permeabilization of mitochondrial membranes for solutes was assessed by high-amplitude mitochondrial swelling. Mitochondrial swelling (a decrease in A550) was recorded using an Infinite 200 plate reader, Tecan, Austria, and 96-well plates. Other details are provided in figures and figure legends.

4.7. Ca^{2+}-Retention Capacity of Mitochondria

Mitochondrial Ca^{2+} uptake and release were recorded in a temperature-controlled electrode chamber using a Ca^{2+}-electrode connected to the computerized recording system, Record 4. The Ca^{2+}-retention capacity was defined as the amount of Ca^{2+} mitochondria taken up in small pulses before the Ca^{2+} release. Mitochondria (1 mg/mL) were added to incubation medium (25 °C) supplemented with 5 mM K^+-succinate plus 2 μg/mL rotenone. Other experimental details are provided in figure legends.

4.8. Measurement of ATP in Mitochondrial Suspension

The ATP content in a suspension of intact mitochondria was determined using an ATP Biomass Kit HS in accordance with the manufacturer's instructions. Incubation medium contained a 20% luciferin-luciferase reagent, 5 mM K^+-succinate, 2 μg/mL of rotenone, 10 μM EGTA, and 0.2 mg of mitochondrial protein/mL. Other experimental details are provided in figures and figure legends. The chemiluminescent signal was calibrated by additions of ATP standards and known amounts of ADP.

4.9. Assessment of the Protonophoric Properties of PIO Using Pyranine-Loaded Vesicles

The luminal pH of liposomes was assayed with pyranine by a slightly modified procedure of [86]. To prepare pyranine-loaded liposomes, a lipid (2 mg POPC, 1 mg POPG, and 1 mg cholesterol) in a chloroform suspension was dried in a round-bottom flask under a stream of nitrogen. The lipid was then resuspended in a buffer (100 mM KCl, 20 mM MES, 20 mM MOPS, 20 mM Tricine titrated with KOH to pH 6.0) containing 0.5 mM pyranine. The suspension was vortexed and then freeze-thawed three times. Unilamellar liposomes were prepared by extrusion through 0.1 μm pore size Nucleopore polycarbonate membranes using an Avanti Mini-Extruder. The unbound pyranine was then removed by passage through a Sephadex G-50 coarse column equilibrated with the same buffer solution. To measure the rate of pH dissipation in liposomes with luminal pH 6.0, liposomes were diluted in a solution buffered to pH 8 and supplemented with 2 mM p-xylene-bis-pyridinium bromide to suppress the fluorescence of leaked pyranine. The inner liposomal pH was estimated from the pyranine fluorescence intensity measured at 505 nm upon excitation at 455 nm with a Panorama Fluorat 02 spectrofluorometer [87]. At the end of each recording, 1 μM lasalocid A was added to dissipate the remaining pH gradient. To prevent the formation of H^+-diffusion potential, the experiments were carried out in the presence of 10 nM valinomycin.

4.10. Assessment of PIO-Dependent Proton Transport in Mitochondria

The rate of proton transport was assessed by the PIO-dependent osmotic swelling of deenergized mitochondria in NH_4NO_3-based medium (135 mM NH_4NO_3, 0.5 mM EGTA, and 10 mM HEPES-KOH (pH 7.0)) [88]. Mitochondrial swelling was defined as a decrease in A_{550} using a plate reader (Infinite 200 Tecan, Austria) and 96-well plates. Other details are provided in figures and figure legends.

4.11. Statistical Analysis

The data shown represent the means ± standard error of means (S.E.M.) or are the means of at least three experiments. Statistical probability (p) values were derived by the Student's t-test.

5. Conclusions

Thus, here, we demonstrated that PIO can behave as a carrier-dependent uncoupler, a regulator of the efficiency of ATP production, and a modulator of the mPTP sensitivity to Ca^{2+} and adenine nucleotides. These properties contribute to both therapeutic and adverse effects of PIO in cells and the organism.

Author Contributions: Conceptualization, K.N.B., Y.N.A., and A.G.K.; investigation, E.S.K., A.B.N., K.N.B., T.I.R., and A.G.K.; writing—original draft preparation, E.S.K., K.N.B., Y.N.A., and A.G.K.; writing—review and editing, E.S.K., Y.N.A., and A.G.K.; visualization, E.S.K. and A.B.N.; supervision and project administration, A.G.K. All authors have read and agreed to the published version of the manuscript.

Funding: This work was supported by a State assignment to the Institute of Theoretical and Experimental Biophysics, Russian Academy of Sciences (ITEB RAS) 075-00381-21-00.

Institutional Review Board Statement: The study was conducted according to the guidelines of the Declaration of Helsinki, and approved by the Commission on Biological Safety and Bioethics of the ITEB RAS (protocol 9/2020, 17 February 2020).

Informed Consent Statement: Not applicable.

Data Availability Statement: Data is contained within the article.

Acknowledgments: We cordially thank Yu. V. Shatalin from the Institute of Theoretical and Experimental Biophysics (Russian Academy of Science) for expert advice.

Conflicts of Interest: The authors declare no conflict of interest.

References

1. Wright, M.B.; Bortolini, M.; Tadayyon, M.; Bopst, M. Minireview: Challenges and opportunities in development of PPAR agonists. *Mol. Endocrinol.* **2014**, *28*, 1756–1768, doi:10.1210/me.2013-1427.
2. Alam, F.; Islam, M.A.; Mohamed, M.; Ahmad, I.; Kamal, M.A.; Donnelly, R.; Idris, I.; Gan, S.H. Efficacy and safety of pioglitazone monotherapy in type 2 diabetes mellitus: A systematic review and meta-analysis of randomised controlled trials. *Sci. Rep.* **2019**, *9*, 5389, doi:10.1038/s41598-019-41854-2.
3. Albert, S.G.; Wood, E.M. Meta-analysis of trials in non-alcoholic fatty liver disease with therapeutic interventions for metabolic syndrome. *Diabetes Metab. Syndr.* **2021**, *15*, 102232, doi:4.10.1016/j.dsx.2021.102232.
4. Lian, J.; Fu, J. Pioglitazone for NAFLD Patients With Prediabetes or Type 2 Diabetes Mellitus: A Meta-Analysis. *Front. Endocrinol.* **2021**, *12*, 615409, doi:10.3389/fendo.2021.615409.
5. Burns, D.K.; Alexander, R.C.; Welsh-Bohmer, K.A.; Culp, M.; Chiang, C.; O'Neil, J.; Evans, R.M.; Harrigan, P.; Plassman, B.L.; Burke, J.R..; et al. Safety and efficacy of pioglitazone for the delay of cognitive impairment in people at risk of Alzheimer's disease (TOMMORROW): A prognostic biomarker study and a phase 3, randomised, double-blind, placebo-controlled trial. *Lancet Neurol.* **2021**, *20*, 537–547, doi:10.1016/S1474-4422(21)00043-0.
6. Hang, X.; Zhang, Y.; Li, J.; Li, Z.; Zhang, Y.; Ye, X.; Tang, Q.; Sun, W. Comparative Efficacy and Acceptability of Anti-inflammatory Agents on Major Depressive Disorder: A Network Meta-Analysis. *Front. Pharmacol.* **2021**, *12*, 691200, doi:10.3389/fphar.2021.691200.
7. Della Pepa, G.; Russo, M.; Vitale, M.; Carli, F.; Vetrani, C.; Masulli, M.; Riccardi, G.; Vaccaro, O.; Gastaldelli, A.; Rivellese, A.A.; et al. Pioglitazone even at low dosage improves NAFLD in type 2 diabetes: Clinical and pathophysiological insights from a subgroup of the TOSCA. IT randomised trial. *Diabetes Res. Clin. Pract.* **2021**, *178*, 108984, doi:10.1016/j.diabres.2021.108984.
8. Zou, G.; Zhou, Z.; Xi, X.; Huang, R.; Hu, H. Pioglitazone Ameliorates Renal Ischemia-Reperfusion Injury via Inhibition of NF-κB Activation and Inflammation in Rats. *Front. Physiol.* **2021**, *12*, 707344, doi:10.3389/fphys.2021.707344.
9. Ramirez-Moral, I.; Lima Ferreira, B.; de Vos, A.F.; van der Poll, T. Post-treatment with the PPAR-γ agonist pioglitazone inhibits inflammation and bacterial growth during Klebsiella pneumonia. *Respir Res.* **2021**, *22*, 230, doi:10.1186/s12931-021-01823-8.
10. Hassan, F.E.; Sakr, H.I.; Mohie, P.M.; Suliman, H.S.; Mohamed, A.S.; Attia, M.H.; Eid, D.M. Pioglitazone improves skeletal muscle functions in reserpine-induced fibromyalgia rat model. *Ann. Med.* **2021**, *53*, 1032–1040, doi:10.1080/07853890.2021.1916069.

11. Yeligar, S.M.; Mehta, A.J.; Harris, F.L.; Brown, L.A.S.; Hart, C.M. Pioglitazone Reverses Alcohol-Induced Alveolar Macrophage Phagocytic Dysfunction. *J. Immunol.* **2021**, *207*, 483–492, doi:10.4049/jimmunol.2000565.
12. Al-Kuraishy, H.M.; Al-Gareeb, A.I.; Alblihed, M.; Guerreiro, S.G.; Cruz-Martins, N.; Batiha, G.E. COVID-19 in Relation to Hyperglycemia and Diabetes Mellitus. *Front. Cardiovasc. Med.* **2021**, *8*, 644095, doi:10.3389/fcvm.2021.644095.
13. Abdelhafez, A.T.; Gomaa, A.M.S.; Ahmed, A.M.; Sayed, M.M.; Ahmed, M.A. Pioglitazone and/or irbesartan ameliorate COPD-induced endothelial dysfunction in side stream cigarette smoke-exposed mice model. *Life Sci.* **2021**, *280*, 119706, doi:10.1016/j.lfs.2021.119706.
14. Gouveia-Eufrasio, L.; Ribeiro, N.Q.; Alves Santos, J.R.; Carvalho da Costa, M.; Peres Emídio, E.C.; Cota de Freitas, G.J.; Fonseca do Carmo, P.H.; Miranda, B.A.; Dornelas de Oliveira, J.C.M.; Vitorino da Silva, L.M.; et al. Randomized, phase 1/2, double-blind pioglitazone repositioning trial combined with antifungals for the treatment of cryptococcal meningitis—PIO study. *Contemp. Clin. Trials Commun.* **2021**, *22*, 100745, doi:10.1016/j.conctc.2021.100745.
15. Weil, Z.M.; Karelina, K.; Whitehead, B.; Velazquez-Cruz, R.; Oliverio, R.; Pinti, M.; Nwafor, D.C.; Nicholson, S.; Fitzgerald, J.A.; Hollander, J.; et al. Mild traumatic brain injury increases vulnerability to cerebral ischemia in mice. *Exp. Neurol.* **2021**, *342*, 113765, doi:10.1016/j.expneurol.2021.113765.
16. DeFronzo, R.A.; Tripathy, D.; Schwenke, D.C.; Banerji, M.; Bray, G.A.; Buchanan, T.A.; Clement, S.C.; Henry, R.R.; Hodis, H.N.; Kitabchi, A.E.; et al. Pioglitazone for diabetes prevention in impaired glucose tolerance. *N. Engl. J. Med.* **2011**, *364*, 1104–1115, doi:10.1056/NEJMoa1010949.
17. de Jong, M.; van der Worp, H.B.; van der Graaf, Y.; Visseren, F.L.J.; Westerink, J. Pioglitazone and the secondary prevention of cardiovascular disease. A meta-analysis of randomized-controlled trials. *Cardiovasc. Diabetol.* **2017**, *16*, 134, doi:10.1186/s12933-017-0617-4.
18. Polyzos, S.A.; Kechagias, S.; Tsochatzis, E.A. Review article: Non-alcoholic fatty liver disease and cardiovascular diseases: Associations and treatment considerations. *Aliment. Pharmacol. Ther.* **2021**, *54*, 1013–1025, doi:10.1111/apt.16575.
19. Nesto, R.W.; Bell, D.; Bonow, R.O.; Fonseca, V.; Grundy, S.M.; Horton, E.S.; Le Winter, M.; Porte, D.; Semenkovich, C.F.; Smith, S.; et al. Thiazolidinedione use, fluid retention, and congestive heart failure: A consensus statement from the American Heart Association and American Diabetes Association. *Diabetes Care* **2004**, *27*, 256–263, doi:10.2337/diacare.27.1.256.
20. Lee, M.Y.; Hsiao, P.J.; Yang, Y.H.; Lin, K.D.; Shin, S.J. The association of pioglitazone and urinary tract disease in type 2 diabetic Taiwanese: Bladder cancer and chronic kidney disease. *PLoS ONE* **2014**, *9*, e85479, doi:10.1371/journal.pone.0085479.
21. McEvoy, G.K. *AHFS Drug Information*, 59th ed.; American Society of Health-System Pharmacists: Bethesda, USA, **2017**; p. 3299.
22. Mehtälä, J.; Khanfir, H.; Bennett, D.; Ye, Y.; Korhonen, P.; Hoti, F. Pioglitazone use and risk of bladder cancer: A systematic literature review and meta-analysis of observational studies. *Diabetol. Int.* **2019**, *10*, 24–36, doi:10.1007/s13340-018-0360-4.
23. Pérez-Ortiz, J.M.; Tranque, P.; Burgos, M.; Vaquero, C.F.; Llopis, J. Glitazones induce astroglioma cell death by releasing reactive oxygen species from mitochondria: Modulation of cytotoxicity by nitric oxide. *Mol. Pharmacol.* **2007**, *72*, 407–417, doi:10.1124/mol.106.032458.
24. Wassef, M.A.E.; Tork, O.M.; Rashed, L.A.; Ibrahim, W.; Morsi, H.; Rabie, D.M.M. Mitochondrial dysfunction in diabetic cardiomyopathy: Effect of mesenchymal stem cell with PPAR-γ agonist or exendin-4. Exp. *Clin. Endocrinol. Diabetes* **2018**, *126*, 27–38, doi:10.1055/s-0043-106859.
25. Kiran, A.V.V.V.R.; Kumari, G.K.; Krishnamurthy, P.T. Preliminary evaluation of anticancer efficacy of pioglitazone combined with celecoxib for the treatment of non-small cell lung cancer. *Investig. New Drugs* **2021**, doi:10.1007/s10637-021-01158-7.
26. Kumari, G.K.; Kiran, A.V.V.V.R.; Krishnamurthy, P.T. Preliminary evaluation on the beneficial effects of pioglitazone in the treatment of endometrial cancer. *Med. Oncol.* **2021**, *38*, 71, doi:10.1007/s12032-021-01521-x.
27. Nesti, L.; Tricò, D.; Mengozzi, A.; Natali, A. Rethinking pioglitazone as a cardioprotective agent: A new perspective on an overlooked drug. *Cardiovasc. Diabetol.* **2021**, *18*, 109, doi:10.1186/s12933-021-01294-7.
28. Butterick, T.A.; Stone, L.H.; Duffy, C.; Holley, C.; Cabrera, J.A.; Crampton, M.; Ward, H.B.; Kelly, R.F.; McFalls, E.O. Pioglitazone increases PGC1-α signaling within chronically ischemic myocardium. *Basic Res. Cardiol.* **2016**, *111*, 37, doi:10.1007/s00395-016-0555-4.
29. Zhang, Z.; Zhang, X.; Meng, L.; Gong, M.; Li, J.; Shi, W.; Qiu, J.; Yang, Y.; Zhao, J.; Suo, Y.; et al. Pioglitazone Inhibits Diabetes-Induced Atrial Mitochondrial Oxidative Stress and Improves Mitochondrial Biogenesis, Dynamics, and Function Through the PPAR-γ/PGC-1α Signaling Pathway. *Front. Pharmacol.* **2021**, *12*, 658362, doi:10.3389/fphar.2021.658362.
30. Lin, Y.Y.Y.; Perez-Polo, J.R.; Birnbaum, Y. Oral glyburide, but not glimepiride, blocks the infarct-size limiting effects of pioglitazone. *Cardiovasc. Drugs Ther.* **2008**, *22*, 429–436, doi:10.1007/s10557-008-6138-3.
31. Wynne, A.M.; Mocanu, M.M.; Yellon, D.M. Pioglitazone mimics preconditioning in the isolated perfused rat heart: A role for the prosurvival kinases PI3K and P42/44MAPK. *J. Cardiovasc. Pharmacol.* **2005**, *46*, 817–822, doi:10.1097/01.fjc.0000188365.07635.57.
32. Ye, Y.; Lin, Y.; Atar, S.; Huang, M.H.; Perez-Polo, J.R.; Uretsky, B.F.; Birnbaum, Y. Myocardial protection by pioglita6zone, atorvastatin, and their combination: Mechanisms and possible interactions. *Am. J. Physiol.* **2006**, *291*, 1158–1169, doi:10.1152/ajpheart.00096.2006.
33. Li, J.; Lang, M.J.; Mao, X.B.; Tian, L.; Feng, Y.B. Antiapoptosis and mitochondrial effect of pioglitazone preconditioning in the ischemic/reperfused heart of rat. *Cardiovasc. Drugs Ther.* **2008**, *22*, 283–291, doi:10.1007/s10557-008-6115-x.

34. Jarrar, Y.B.; Jarrar, Q.; Abaalkhail, S.J.; Kalloush, H.M.; Naser, W.; Zihlif, M.; Shhab, M.A.; Madani, A.E.; Jamous, Y.; Lee, S.J. Molecular toxicological alterations in the mouse hearts induced by sub-chronic thiazolidinedione drugs administration. *Fundam Clin Pharmacol.* **2021**, doi:10.1111/fcp.12694.
35. Salem, A.F.; Whitaker-Menezes, D.; Howell, A.; Sotgia, F.; Lisanti, M.P. Mitochondrial biogenesis in epithelial cancer cells promotes breast cancer tumor growth and confers autophagy resistance. *Cell Cycle* **2012**, *11*, 4174–4180, doi:10.4161/cc.22376.
36. Rezaiean Mehrabadi, A.; Jamshidzadeh, A.; Rashedinia, M.; Niknahad, H. Study of the effects of ATP suppliers and thiol reductants on toxicity of pioglitazone in isolated rat liver mitochondria. *Iran. J. Pharm. Res.* **2015**, *14*, 825–832.
37. Woo, M.; Kim, M. Insulin sensitization causes accelerated sinus nodal dysfunction through autophagic dysregulation in hypertensive mice. *Transl. Clin. Pharmacol.* **2021**, *29*, 92–106, doi:10.12793/tcp.2021.29.e9.
38. Colca, J.R.; McDonald, W.G.; Waldon, D.J.; Leone, J.W.; Lull, J.M.; Bannow, C.A.; Lund, E.T.; Mathews, W.R. Identification of a novel mitochondrial protein ("mitoNEET") cross-linked specifically by a thiazolidinedione photoprobe. *Am. J. Physiol.* **2004**, *286*, 252–260, doi:10.1152/ajpendo.00424.2003.
39. Mons, C.; Botzanowski, T.; Nikolaev, A.; Hellwig, P.; Cianférani, S.; Lescop, E.; Bouton, C.; Golinelli-Cohen, M.P. The H2O2-resistant Fe-S redox switch mitoNEET acts as a pH sensor to repair stress-damaged Fe-S protein. *Biochemistry* **2018**, *57*, 5616–5628, doi:10.1021/acs.biochem.8b00777.
40. Tamir, S.; Paddock, M.L.; Darash-Yahana-Baram, M.; Holt, S.H.; Sohn, Y.S.; Agranat, L.; Michaeli, D.; Stofleth, J.T.; Lipper, C.H.; Morcos, F.; et al. Structure-function analysis of NEET proteins uncovers their role as key regulators of iron and ROS homeostasis in health and disease. *Biochim. Biophys. Acta* **2015**, *1853*, 1294–1315, doi:10.1016/j.bbamcr.2014.10.014.
41. Yuan, H.; Li, X.; Zhang, X.; Kang, R.; Tang, D. CISD1 inhibits ferroptosis by protection against mitochondrial lipid peroxidation. *Biochem. Biophys. Res. Commun.* **2016**, *478*, 838–844, doi:10.1016/j.bbrc.2016.08.034.
42. Vernay, A.; Marchetti, A.; Sabra, A.; Jauslin, T.N.; Rosselin, M.; Scherer, P.E.; Demaurex, N.; Orci, L.; Cosson, P. MitoNEET-dependent formation of intermitochondrial junctions. *Proc. Natl. Acad. Sci. USA* **2017**, *114*, 8277–8282, doi:10.1073/pnas.1706643114.
43. Wiley, S.E.; Murphy, A.N.; Ross, S.A.; van der Geer, P.; Dixon, J.E. MitoNEET is an iron-containing outer mitochondrial membrane protein that regulates oxidative capacity. *Proc. Natl. Acad. Sci. USA* **2007**, *104*, 5318–5323, doi:10.1073/pnas.0701078104.
44. Lipper, C.H.; Karmi, O.; Sohn, Y.S.; Darash-Yahana, M.; Lammert, H.; Song, L.; Liu, A.; Mittler, R.; Nechushtai, R.; Onuchic, J.N.; et al. Structure of the human monomeric NEET protein MiNT and its role in regulating iron and reactive oxygen species in cancer cells. *Proc. Natl. Acad. Sci. USA* **2018**, *115*, 272–277, doi:10.1073/pnas.1715842115.
45. Sohn, Y.S.; Tamir, S.; Song, L.; Michaeli, D.; Matouk, I.; Conlan, A.R.; Harir, Y.; Holt, S.H.; Shulaev, V.; Paddock, M.L.; et al. NAF-1 and mitoNEET are central to human breast cancer proliferation by maintaining mitochondrial homeostasis and promoting tumor growth. *Proc. Natl. Acad. Sci. USA* **2013**, *110*, 14676–14681, doi:10.1073/pnas.1313198110.
46. Kusminski, C.M.; Chen, S.; Ye, R.; Sun, K.; Wang, Q.A.; Spurgin, S.B.; Sanders, P.E.; Brozinick, J.T.; Geldenhuys, W.J.; Li, W.H.; et al. MitoNEET-Parkin effects in pancreatic alpha- and beta-cells, cellular survival, and intrainsular cross talk. *Diabetes* **2016**, *65*, 1534–1555, doi:10.2337/db15-1323.
47. Kusminski, C.M.; Holland, W.L.; Sun, K.; Park, J.; Spurgin, S.B.; Lin, Y.; Askew, G.R.; Simcox, J.A.; McClain, D.A.; Li, C.; et al. MitoNEET-driven alterations in adipocyte mitochondrial activity reveal a crucial adaptive process that preserves insulin sensitivity in obesity. *Nat. Med.* **2012**, *18*, 1539–1549, doi:10.1038/nm.2899.
48. Kusminski, C.M.; Park, J.; Scherer, P.E. MitoNEET-mediated effects on browning of white adipose tissue. *Nat. Commun.* **2014**, *5*, 3962, doi:10.1038/ncomms4962.
49. Raddock, M.L.; Wiley, S.E.; Axelrod, H.L.; Cohen, A.E.; Roy, M.; Abresch, E.C.; Capraro, D.; Murphy, A.N.; Nechushtai, R.; Dixon, J.E.; et al. MitoNEET is a uniquely folded 2Fe 2S outer mitochondrial membrane protein stabilized by pioglitazone. *Proc. Natl. Acad. Sci. U. S. A.* **2007**, *104*, 14342–14347, doi:10.1073/pnas.0707189104.
50. Zuris, J.A.; Harir, Y.; Conlan, A.R.; Shvartsman, M.; Michaeli, D.; Tamir, S.; Paddock, M.L.; Onuchic, J.N.; Mittler, R.; Cabantchik, Z.I.; et al. Facile transfer of [2Fe-2S] clusters from the diabetes drug target mitoNEET to an apo-acceptor protein. *Proc. Natl. Acad. Sci. USA* **2011**, *108*, 13047–13052, doi:10.1073/pnas.1109986108.
51. Tarze, A.; Deniaud, A.; Le Bras, M.; Maillier, E.; Molle, D.; Larochette, N.; Zamzami, N.; Jan, G.; Kroemer, G.; Brenner, C. GAPDH, a novel regulator of the pro-apoptotic mitochondrial membrane permeabilization, *Oncogene* **2007**, *26*, 2606–2620, doi:10.1038/sj.onc.1210074.
52. Bénit, P.; Pelhaître, A.; Saunier, E.; Bortoli, S.; Coulibaly, A.; Rak, M.; Schiff, M.; Kroemer, G.; Zeviani, M.; Rustin, P.E. Paradoxical inhibition of glycolysis by pioglitazone opposes the mitochondriopathy caused by AIF deficiency. *BioMedicine* **2017**, *17*, 75–87, doi:10.1016/j.ebiom.2017.02.013.
53. García-Ruiz, I.; Solís-Muñoz, P.; Fernández-Moreira, D.; Muñoz-Yagüe, T.; Solís-Herruzo, J.A. Pioglitazone leads to an inactivation and disassembly of complex I of the mitochondrial respiratory chain. *BMC Biol.* **2013**, *11*, 88, doi:10.1186/1741-7007-11-88.
54. Sanz, M.N.; Sánchez-Martín, C.; Detaille, D.; Vial, G.; Rigoulet, M.; El-Mir, M.Y.; Rodríguez-Villanueva, G. Acute mitochondrial actions of glitazones on the liver: A crucial parameter for their antidiabetic properties. *Cell Physiol. Biochem.* **2011**, *28*, 899–910, doi:10.1159/000335804.
55. Geldenhuys, W.J.; Funk, M.O.; Barnes, K.F.; Carroll, R.T. Structure-based design of a thiazolidinedione which targets the mitochondrial protein mitoNEET. *Bioorg. Med. Chem. Lett.* **2010**, *20*, 819–823, doi:10.1016/j.bmcl.2009.12.088.

56. Sato, T.; Takemura, A.; Ito, K. Role of respiratory uncoupling in drug-induced mitochondrial permeability transition. *Toxicol. Appl. Pharmacol.* **2021**, *15*, 115659, doi:10.1016/j.taap.2021.115659.
57. Pruimboom-Brees, I.M.; Francone, O.; Pettersen, J.C.; Kerlin, R.L.; Will, Y.; Amacher, D.E.; Boucher, G.G.; Morton, D. The development of subcutaneous sarcomas in rodents exposed to peroxisome proliferators agonists: Hypothetical mechanisms of action and de-risking attitude. *Toxicol. Pathol.* **2012**, *40*, 810–818, doi:10.1177/0192623312441406.
58. Shannon, C.E.; Daniele, G.; Galindo, C.; Abdul-Ghani, M.A.; DeFronzo, R.A.; Norton, L. Pioglitazone inhibits mitochondrial pyruvate metabolism and glucose production in hepatocytes. *FEBS J.* **2017**, *284*, 451–465, doi:10.1111/febs.13992.
59. O'Neil, M.J. *The Merck Index—An Encyclopedia of Chemicals, Drugs, and Biologicals*, 15th ed.; Royal Society of Chemistry: Cambridge, UK, 2013; p. 1477.
60. McLaughlin, S.G.; Dilger, J.P. Transport of protons across membranes by weak acids. *Physiol. Rev.* **1980**, *60*, 825–863, doi:10.1152/physrev.1980.60.3.825.
61. Dubinin, M.V.; Khoroshavina, E.I.; Samartsev, V.N. Lithocholic acid induces two different calcium-dependent inner membrane permeability systems in liver mitochondria. *Biochemistry (Moscow), Supplement Series A: Membrane and Cell Biology* **2017**, *11*, 231–236, doi:10.1134/S1990747817030059.
62. Kharechkina, E.S.; Nikiforova, A.B.; Teplova, V.V.; Odinokova, I.V.; Krestinina, O.V.; Baburina, Y.L.; Kruglova, S.A.; Kruglov, A.G. Regulation of permeability transition pore opening in mitochondria by external NAD(H). *Biochim. Biophys. Acta Gen. Subj.* **2019**, *1863*, 771–783, doi:10.1016/j.bbagen.2019.01.003.
63. Hagen, T.; Lagace, C.J.; Modica-Napolitano, J.S.; Aprille, J.R. Permeability transition in rat liver mitochondria is modulated by the ATP-Mg/Pi carrier. *Am. J. Physiol.* **2003**, *285*, 274–281 doi:10.1152/ajpgi.00052.2003.
64. Andreyev, A.Yu.; Bondareva, T.O.; Dedukhova, V.I.; Mokhova, E.N.; Skulachev, V.P.; Tsofina, L.M.; Volkov, N.I.; Vygodina, T.V. The ATP/ADP-antiporter is involved in the uncoupling effect of fatty acids on mitochondria. *Eur. J. Biochem.* **1989**, *182*, 585–592, doi:10.1111/j.1432-1033.1989.tb14867.x.
65. Žuna K.; Jovanović, O.; Khailova, L.S.; Škulj, S.; Brkljača, Z.; Kreiter, J.; Kotova, E.A.; Vazdar, M.; Antonenko, Yu, N.; Pohl, E.E. Mitochondrial Uncoupling Proteins (UCP1-UCP3) and Adenine Nucleotide Translocase (ANT1) Enhance the Protonophoric Action of 2,4-Dinitrophenol in Mitochondria and Planar Bilayer Membranes. *Biomolecules* **2021**, *11*, 1178, doi:10.3390/biom11081178.
66. Berardi, J.M.; Chou, J.J. Fatty acid flippase activity of UCP2 is essential for its proton transport in mitochondria. *Cell Metab.* **2014**, *20*, 541–552, doi:10.1016/j.cmet.2014.07.004.
67. Seedher, N.; Kanojia, M. Co-solvent solubilization of some poorly-soluble antidiabetic drugs. *Pharm Dev. Technol,* **2009**, *14*, 185–192, doi:10.1080/10837450802498894.
68. Wong, L.H.; Gatta, A.T.; Levine, T.P. Lipid transfer proteins: The lipid commute via shuttles, bridges and tubes. *Nat. Rev. Mol Cell Biol.* **2019**, *20*, 85–101, doi:10.1038/s41580-018-0071-5.
69. Geisler, J.G. 2,4 Dinitrophenol as Medicine. *Cells* **2019**, *8*, 280, doi:10.3390/cells8030280.
70. Hamilton, J.A.; Johnson, R.A.; Corkey, B.; Kamp, F. Fatty acid transport: The diffusion mechanism in model and biological membranes. *J. Mol. Neurosci.* **2001**, *16*, 99–108; discussion 151–157, doi:10.1385/JMN:16:2-3:99.
71. Brustovetsky, N.N.; Dedukhova, V.I.; Egorova, M.V.; Mokhova, E.N.; Skulachev, V.P. Inhibitors of the ATP/ADP antiporter suppress stimulation of mitochondrial respiration and H+ permeability by palmitate and anionic detergents. *FEBS* **1990**, *272*, 187–189, doi:10.1016/0014-5793(90)80480-7.
72. Brustovetsky, N.; Klingenberg, M. The reconstituted ADP/ATP carrier can mediate H+ transport by free fatty acids, which is further stimulated by mersalyl. *J. Biol. Chem.* **1994**, *269*, 27329–27336, doi:10.1016/S0021-9258(18)46989-X.
73. Bertholet, A.M.; Kirichok, Y. UCP1: A transporter for H+ and fatty acid anions. *Biochimie* **2017**, *134*, 28–34, doi:10.1016/j.biochi.2016.10.013.
74. Bernardi, P.; Broekemeier, K.M.; Pfeiffer, D.R. Recent progress on regulation of the mitochondrial permeability transition pore; a cyclosporin-sensitive pore in the inner mitochondrial membrane. *J. Bioenerg. Biomembr.* **1994**, *26*, 509–517, doi:10.1007/BF00762735.
75. Traba, J.; del Arco, A.; Duchen, M.R.; Szabadkai, G.; Satrústegui, J. SCaMC-1 promotes cancer cell survival by desensitizing mitochondrial permeability transition via ATP/ADP-mediated matrix Ca(2+) buffering. *Cell Death Differ.* **2012**, *19*, 650–660, doi:10.1038/cdd.2011.139.
76. Ramakrishna, K.; Rebecca Shiffali, D.; Pani Kumar, A.D. Estimation of Pioglitazone Hydrochloride in Bulk Drug and Pharmaceutical Dosage Forms by Hydrotropy Technique and Oxidative-Coupling Reaction. *Asian, J. Research Chem.* **2013**, *6*, 172–176.
77. Khailova, L.S.; Firsov, A.M.; Kotova, E.A.; Antonenko, Y.N. Interaction of Potent Mitochondrial Uncouplers with Thiol-Containing Antioxidants. *Antioxidants* **2019**, *8*, 194, doi:10.3390/antiox8060194.
78. Saremi, A.; Schwenke, D.C.; Buchanan, T.A.; Hodis, H.N.; Mack, W.J.; Banerji, M.; Bray, G.A.; Clement, S.C.; Henry, R.R.; Kitabchi, A.E.; et al. Pioglitazone slows progression of atherosclerosis in prediabetes independent of changes in cardiovascular risk factors. *Arterioscler. Thromb. Vasc. Biol.* **2013**, *33*, 393–399, doi:10.1161/ATVBAHA.112.300346.
79. Caldeira da Silva, C.C.; Cerqueira, F.M.; Barbosa, L.F.; Medeiros, M.H.; Kowaltowski, A.J. Mild mitochondrial uncoupling in mice affects energy metabolism, redox balance and longevity. *Aging Cell* **2008**, *7*, 552–560, doi:10.1111/j.1474-9726.2008.00407.x.
80. Perry, R.J.; Zhang, D.; Zhang, X.M.; Boyer, J.L.; Shulman, G.I. Controlled-release mitochondrial protonophore reverses diabetes and steatohepatitis in rats. *Science* **2015**, *347*, 1253–1256, doi:10.1126/science.aaa0672.

81. Johnson, D.; Lardy, H.A. Isolation of liver or kidney mitochondria. *Methods Enzymol.* **1967**, *10*, 94–96, doi:10.1016/0076-6879(67)10018-9.
82. Nikiforova, A.B.; Saris, N.E.; Kruglov, A.G. External mitochondrial NADH-dependent reductase of redox cyclers: VDAC1 or Cyb5R3? *Free Radic. Biol. Med.* **2014**, *74*, 74–84, doi:10.1016/j.freeradbiomed.2014.06.005.
83. Gornall, A.G.; Bardawill, C.J.; David, M.M. Determination of serum proteins by means of the biuret reaction. *J. Biol. Chem.* **1949**, *177*, 751–766.
84. Chinopoulos, C.; Vajda, S.; Csanády, L.; Mándi, M.; Mathe, K.; Adam-Vizi, V. A novel kinetic assay of mitochondrial ATP-ADP exchange rate mediated by the ANT. *Biophys. J.* **2009**, *96*, 2490–2504, doi:10.1016/j.bpj.2008.12.3915.
85. Dubinin, M.V.; Semenova, A.A.; Ilzorkina, A.I.; Penkov, N.V.; Nedopekina, D.A.; Sharapov, V.A.; Khoroshavina, E.I.; Davletshin, E.V.; Belosludtseva, N.V.; Spivak, A.Y.; et al. Mitochondria-targeted prooxidant effects of betulinic acid conjugated with delocalized lipophilic cation F16. *Free Radic Biol Med.* **2021**, *168*, 55–69, doi:10.1016/j.freeradbiomed.2021.03.036.
86. Chen, Y.; Schindler, M.; Simon, S.M. A mechanism for tamoxifen-mediated inhibition of acidification. *J. Biol. Chem.* **1999**, *274*, 18364–18373, doi:10.1074/jbc.274.26.18364.
87. Denisov, S.S.; Kotova, E.A.; Khailova, L.S.; Korshunova, G.A.; Antonenko, Y.N. Tuning the hydrophobicity overcomes unfavorable deprotonation making octylamino-substituted 7-nitrobenz-2-oxa-1,3-diazole (n-octylamino-NBD) a protonophore and uncoupler of oxidative phosphorylation in mitochondria. *Bioelectrochemistry* **2014**, *98*, 30–38, doi:10.1016/j.bioelechem.2014.02.002.
88. Brierley, G.P.; Jurkowitz, M.; Scott, K.M.; Merola, A.J. Ion transport by heart mitochondria. XX. Factors affecting passive osmotic swelling of isolated mitochondria. *J. Biol. Chem.* **1970**, *245*, 5404–5411.